Electrochemical Insertion/extraction of Lithium in Multiwall Carbon Nanotube/Sb and $SnSb_{0.5}$ Nanocomposites

Wei Xiang Chen, Jim Yang Lee and Zhaolin Liu

***Abstract*—Multiwall carbon nanotubes (CNTs) were synthesized by catalytic chemical vapor deposition of acetylene and used as templates to prepare CNT-Sb and CNT-$SnSb_{0.5}$ nanocomposites via the chemical reduction of $SnCl_2$ and $SbCl_3$ precursors. SEM and TEM imagings show that the Sb and $SnSb_{0.5}$ particles were uniformly dispersed in the CNT web and on the outside surface of CNTs. These CNT-metal composites are active anode materials for lithium ion batteries, showing improved cyclability compared to unsupported Sb and SnSb particles; and higher reversible specific capacities than CNTs. The improvement in cyclability may be attributed to the nanoscale dimensions of the metal particles and CNT's role as a buffer in containing the mechanical stress arising from the volume changes in electrochemical lithium insertion and extraction reactions.**

***Index Terms*—Carbon nanotubes, SnSb alloy, Composite, Anode materials, Li-ion batteries.**

I. Introduction

CARBON nanotubes (CNTs) are one-dimensional nanoscale materials which are micrometers in lengths and nanometers in diameters. CNTs can offer many significant advantages over existing materials [1, 2], and have been suggested for a diverse range of applications such as nanoscale electronic devices [3, 4], hydrogen storage [5, 6], composite making [7, 8] and electrochemical energy conversions [9-14]. CNTs are interesting one-dimensional host for the intercalation of Li and other alkali metals. Nalimova *et al* [15] reported that multiwalled carbon nanotubes could accommodate a very high Li concentration in an argon atmosphere under high-pressures. Electrochemical lithium intercalation into CNTs was also possible [9-12]. These investigations invariably confirmed the presence of lithium in CNTs and a capacity dependence on the microstructures of the CNTs. Reversible capacities in the range of 80-640 mAh/g were reported. Gao *et al* [10] showed that single-wall carbon nanotubes (SWNTs) could have higher reversible capacities between 450 and 600 mAh/g. Ballmilling of SWNTs was able to further increase the capacity from 600 mAh/g to 1000 mAh/g.

On the other hand, metals such as Al, Sn, Sb, Pb are able to store Li *via* alloy formation through electrochemical means resulting in capacities substantially higher than those of the carbonaceous materials. However, a large specific volume change also occurs during Li insertion and extraction reactions, causing the electrode to fail by pulverization. As a result rapid capacity fading is observed [16]. In order to improve structural stability, superfine alloys, intermetallic compounds and active/inactive composite alloy materials, such as Sn-Sb [17, 18], Cu-Sn [19], Co-Sb [20] and Fe-Sn-C [21] systems, have been developed and investigated. In general, superfine or nanoscale active materials are expected to have less specific volume variations and hence better cyclability in electrochemical intercalation and extraction of lithium ions [22, 23]. Li *et al* [24, 25] reported high capacity and good cyclability for nanostructured tin oxides prepared by the templating technique. Similarly, Yang *et al* [17, 18] found that ultrafine Sn-SnSb particles with d_p <300 nm could substantially improve the electrochemical performance of the tin based alloys. On the other hand superfine or nanosize active materials of Sn-Sb, Ag and Sb are predisposed to particle aggregation, and micrometer size particles were formed during lithation and de-lithation reactions [26, 27]. Aggregation is perceived to be the primary cause for the observed gradual decline in the lithium storage capacity. The problem is more subdue in composites such as Si-C [28], Sn-C [29] and Sn-Fe-C [21]. Investigations by Shi *et al* [30] showed that the dispersion of nanosize Sn-Sb alloy particles on the surface of mesophase carbon microbeads (MCMB) could enhance the cycling performance while maintaining a high reversible capacity. In their views, the stability of the nanosize Sn-Sb alloy particles is greatly improved in the MCMB environment [30]. Similarly, our previous investigations have also shown that high dispersions of tin oxide on graphite are superior to pristine tin oxide in cycle efficiency [31, 32].

In the present study, we undertook the synthesis of nanoscale Sb and $SnSb_{0.5}$ alloy particles using CNTs as the templates; and evaluated the suitability of the resulting composites as anode

Wei Xiang Chen is with Singapore-MIT Alliance, National University of Singapore, 4 Engineering Drive 3, Singapore 117576 (e-mail: smacwx@nus.edu.sg).

Jim Yang Lee is with Singapore-MIT Alliance, Department of Chemical and Environmental Engineering, and Institute of Materials Research and Engineering, National University of Singapore, 10 Kent Ridge Crescent, Singapore 119260 (e-mail: cheleejy@nus.edu.sg).

Zhaolin Liu is with Institute of Materials Research and Engineering, 3 Research Link, Singapore 117602 (e-mail: zl-liu@imre.org.sg).

materials in Li ion batteries. As all constituents of the new composites are active host materials for Li ion storage and retrieval, it is expected that the CNT-metal nanocomposites should exhibit improvements in both the cyclability and capacity.

II. Experimental Details

A. Preparation of carbon nanotubes

Carbon nanotubes were synthesized by the decomposition of C_2H_2 using cobalt nanoparticles supported on SiO_2 as the catalyst. The cobalt catalyst was distributed uniformly over the bottom of a quartz combustion boat, which was placed centrally in a horizontal quartz process tube. A mixture of C_2H_2 and N_2, with flow rates of 100 mL/min and 500 mL/min respectively, was allowed to pass over the catalyst surface at 750°C for 15 min. At the end of reaction, the catalyst was removed from the resulting solid mass by treatment with concentrated nitric acid and hydrofluoric acid in sequence. The remaining solid was filtered off, washed with distilled water, and dried at 120•. The CNT samples were characterized by transmission electron microscopy (TEM, on a JEOL JEM 2010) and X-ray diffraction (XRD, on a Philips X Pert MPD).

B. Preparation of CNT-metal nanocomposites

The composites of CNT and Sb or $SnSb_{0.5}$ were prepared by chemical reduction of the metal chloride salts in suspensions of CNT. Typically, calculated amounts of $SnCl_2$ and $SbCl_3$ were dissolved in distilled water to obtain a solution with 0.06M Sn^{2+} and 0.02M Sb^{3+}. A measured volume of the solution was transferred to a conical flask where it was further diluted by about 150 mL of distilled water; followed by the addition of 0.1000 g of CNT. After the suspension was sonicated for 2 h, 100 mL of alkaline KBH_4 solution was introduced in drop-wise fashion. Twice the stoichiometric amount of KBH_4 needed for metal ion reduction was used. During the addition of the reducing agent the CNT suspension was subjected to vigorous mechanical agitation. The CNT-metal nanocomposites were then filtered off, washed with copious amount of water, rinsed with acetone, and vacuum dried overnight at 120°C. Unsupported Sb and Sn-Sb particles were prepared by the same procedures but in the absence of CNTs. The morphology of the composites was examined by scanning electron microscopy (SEM, on a JEOL JSM-5600LV) and TEM (on a JEOL JEM 2010). Elemental analysis using ICP-AES showed Sn:Sb ratios of 1:0.52 and 1:0.47 for CNT-supported and unsupported Sn-Sb alloys respectively.

C. Electrochemical measurements

The electrochemical behaviors of CNTs and CNT-metal nanocomposites in Li^+ insertion and extraction reactions were measured by a Maccor series 2000 battery tester, using a constant current density of 50 mA/g and a voltage range of 0-2.0V at room temperature. The working electrode consisted of the active material with 10 wt.% each of acetylene black and PVDF used as conductivity enhancer and binder respectively. Half-cells with Li disks as counter electrodes were assembled in a M Braun M150 Ar filled glove box which maintained the moisture and oxygen contents at less than 1 ppm each. Microporous polypropylene films (Celgard 2400) were used as the separator and a 1 M $LiPF_6$ solution in a 1:1 v/v mixture of ethylene carbonate (EC) and diethyl carbonate (DEC) was used as the electrolyte.

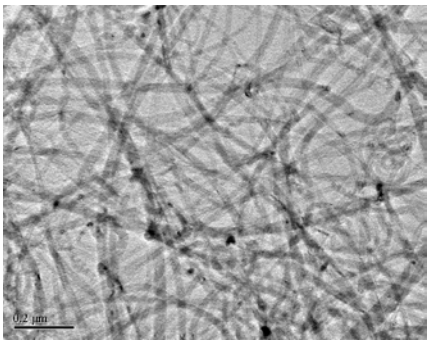

Fig. 1. TEM image of carbon nanotubes.

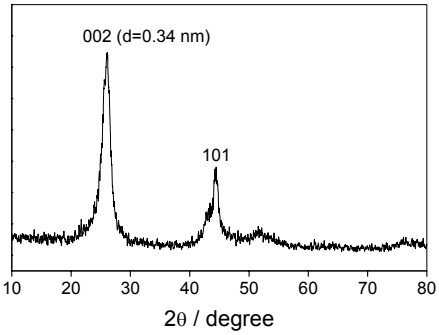

Fig. 2. XRD patterns of carbon nanotubes

III. Results And Discussion

A. Structure of CNTs

The TEM image of CNTs in Fig. 1, which shows a web of hollow tubes with outer diameters between 20 and 40 nm, are characteristic of a multi-wall CNT structure. The XRD pattern of the CNTs is shown in Fig. 2. The sharpness of the (002) diffraction peak indicates that the CNTs were well-graphitized, with a d_{002} spacing of 0.34nm calculated according to the Bragg's equation.

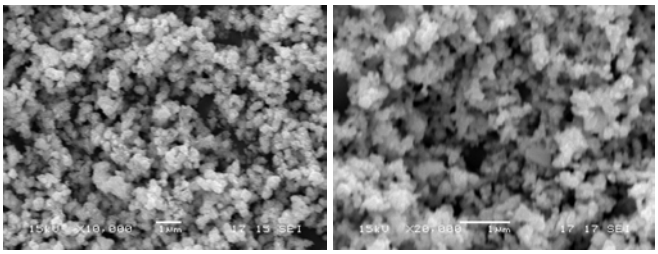

(a) (b)

Fig. 3. SEM images of (a) Sb and (b) $SnSb_{0.5}$ alloy particles.

B. SEM and TEM images of nanostructured CNT-metal composites

The SEM images of unsupported Sb and $SnSb_{0.5}$ in Fig. 3 show particles in the range of 200-300 nm for the former and 150-200 nm for the latter. These should be compared with the SEM and TEM images of CNT-Sb and CNT-$SnSb_{0.5}$ in Fig. 4. For the CNT-Sb nanocomposite, most of the Sb appeared as a 20 nm semi-continuous coating on the CNT walls. In the case of CNT-$SnSb_{0.5}$ nanocomposite, the CNT web captured a large fraction of particles 100 to 200 nm in diameters. The particles that were directly deposited on the outer surface of the CNTs were much smaller, with diameters typically in the range of 10-30 nm. In a related work, Zhang *et al* [33] investigated the deposition of various metals on suspended carbon nanotubes by electron-beam evaporation. They found that the coatings of Ti, Ni and Pd on CNTs were either continuous or quasi-continuous. The observation was in sharp contrast to the deposition of Au, Al and Fe, which could only form isolated particles on the CNT surface. The apparent difference in the adhesion characteristics of Sb and $SnSb_{0.5}$ to CNT can likewise be attributed to the different nature of interactions between CNT and these metals. This is most succinctly illustrated by the TEM images in Fig. 4(b) and (d).

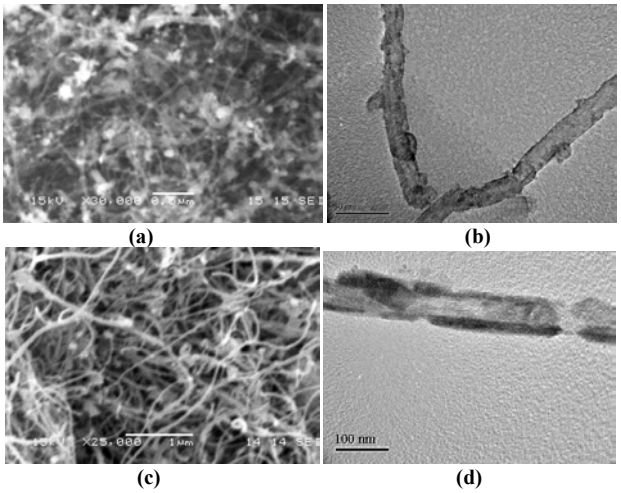

Fig. 4. SEM and TEM images of CNTs-metal nanocomposites. (a) SEM and (b) TEM of CNT-$SnSb_{0.5}$, (c) SEM and (d) TEM of CNT-Sb.

C. Electrochemical charge-discharge performances of CNTs and CNT-metal nanocomposite electrodes

Fig. 5(a) shows the discharge and recharge curves of a pristine CNT electrode for the first three cycles. A voltage plateau at about 0.75 V appeared in the first discharge (lithiation) cycle, which is often associated with electrolyte decomposition and the formation of a solid electrolyte interface (SEI). A very large Li-insertion capacity of 822 mAh/g was obtained in the first discharge cycle, out of which only 200 mAh/g could be recovered in the next and subsequent recharge cycles where Li^+ de-insertion took place. The large first cycle irreversible capacity loss of 622 mAh/g could be attributed to various causes such as the reduction of dioxygen molecules or oxygenated functional groups on the CNT surface [5], and the abovementioned formation of SEI on the CNT surface. These reactions, which occur at potentials higher than 1.5V and at 0.75 V respectively in the first discharge cycle, contributed collectively to the large first cycle lithiation capacity. The reversible capacity of 200 mAh/g was lower than the values reported by others [5,10]. The difference could be due to the lower cut-off voltage used in this study (2.0 V). When the cut-off potential was raised to 2.8 or 3.0V as in [5, 10], the reversible capacity was increased to about 300 mAh/g.

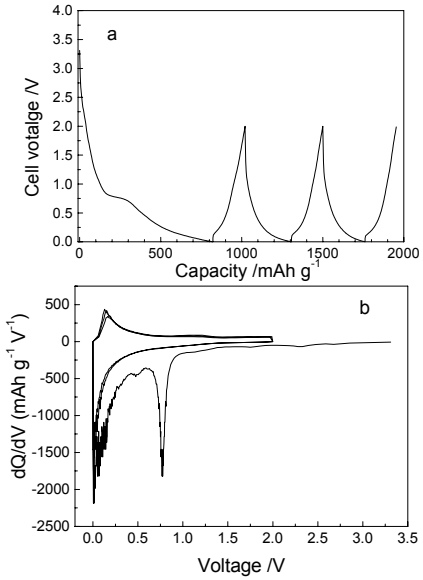

Fig. 5. (a) Voltage *vs.* capacity and (b) differential capacity vs. voltage curves of CNT electrodes for the first three cycle. The charge-discharge current density was 50 mA/g.

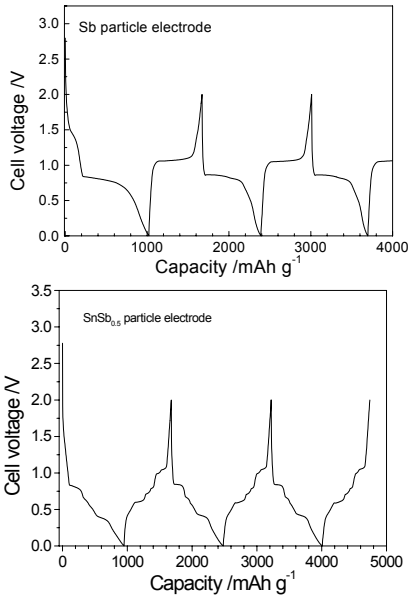

Fig. 6. The voltage *vs.* capacity profiles of Sb and $SnSb_{0.5}$ electrodes obtained . at a charge-discharge current density of 50 mA/g.

A differential capacity plot (plot of dQ/dV vs. potential) was generated based on the data in Fig. 5(a) to better resolve the processes in electrochemical lithiation and de-lithiation. A sharp peak corresponding to the formation of SEI was found at ~0.75 V (Fig 5(b)), which expectedly disappeared in

subsequent cycles. Lithium extraction occurred throughout the region of 0-2V, and was marked by the anodic peak at ~0.2 V. Such large voltage hysteresis is not uncommon among CNT materials, but the cause remains unexplained. This deficiency has greatly undermined the value of CNTs as anode materials of Li-ion batteries.

The discharge and recharge curves for Sb and $SnSb_{0.5}$ alloy electrodes in the first few cycles are given in Fig. 6, from which the reversible capacities for Sb and $SnSb_{0.5}$ were calculated to be 648 mAh/g and 728 mAh/g respectively. These values are much higher than the capacities of most CNTs and the theoretical value of 372 mAh/g for crystalline carbonaceous materials. The potential plateau at ~0.8 V in the discharge curve of Sb was very likely due to the reaction: $Sb + Li^+ + 3e^- \rightarrow Li_3Sb$ [16]. It is well known that there are several voltage plateaus in the lithiation and de-lithiation of Sn and Sn-based alloys. The potential profiles in Fig. 6(b) for the $SnSb_{0.5}$ alloy electrode are replete with a large number of voltage plateaus, a characteristic of multiphase materials where different active phases of the alloy react with lithium at different potentials. The voltage plateau at ~0.8 V in Fig. 6(b) in the discharge curve corresponds well with the start of the SnSb alloying reaction with lithium. It has been established by *ex situ* XRD that SnSb, as well as multiphase Sn/SnSb system, first reacts with lithium according to the reaction: $SnSb + 3Li^+ + 3e^- \rightarrow Li_3Sb + Sn$ [16]. After the formation of Li_3Sb is completed, the Sn active phase reacts further with lithium, yielding Li-Sn alloys of different compositions (Li_xSn_y) in stages depending on the prevailing voltage. The voltage plateaus at 0.7V and 0.6V in Fig. 6, commonly associated with Li_2Sn_5 and LiSn formations, are not as visibly detectable as the voltage plateau at 0.4 V for Li_7Sn_3 formation [16]. Below 0.4 V, the lithium content in the alloy continues to enrich, from Li_5Sn_2 to a final stoichiometry of $Li_{22}Sn_5$ [16].

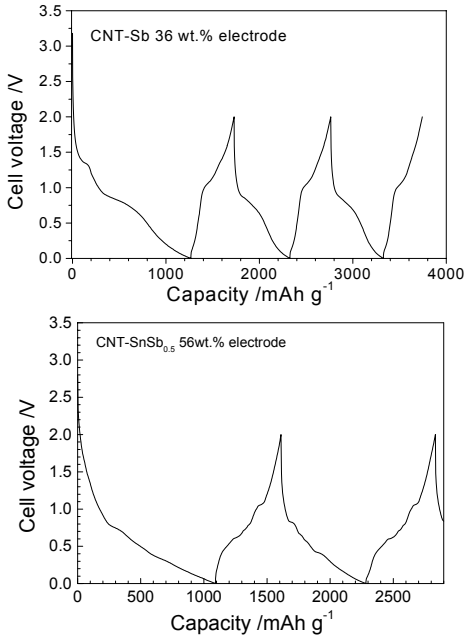

Fig. 7. The voltage *vs.* capacity curves of CNT-Sb and CNT-$SnSb_{0.5}$ nanocomposite electrodes. The charge-discharge current density is 50 mA/g.

Fig. 7 shows the voltage profiles of CNT-36 wt.% Sb and CNT-56 wt.% $SnSb_{0.5}$ in the first two cycles of lithiation and de-lithiation. As CNT, Sb and $SnSb_{0.5}$ are all active towards Li storage, the reversible capacities of these CNT-metal composites could be as high as 462 and 518 mAh/g, respectively. The capacities in first cycle electrochemical Li insertion and extraction reactions are summarized in Table 1. It was found that the reversible capacities of CNT-metal composites were slightly higher than the weighted sums of the specific capacities of CNTs and metals. This capacity augmentation is likely due to the better utilization of the Li storage metal in the CNT-metal composites. In our previous work, a similar synergy in capacity existed between graphite and tin oxide [31,32]. The exact nature of such interactions between carbon and metal and their implications has yet to be understood. Nevertheless, Table I shows that the first cycle coulombic efficiency had improved substantially from 24 % for CNT to 36.5% in CNT-36 wt.% Sb and 47% in CNT-56 wt.% $SnSb_{0.5}$. However, the large first cycle irreversible capacity loss was not abated in these systems. It is tempting to attribute the large irreversible capacity loss to SEI formation and other irreversible processes occurring on the surface of the CNTs and metal/alloy particles.

TABLE I
COMPARISON OF CAPACITIES IN FIRST CYCLE LI INSERTION AND EXTRACTION REACTIONS

Electrode	1st Li-insertion /mAh g^{-1}	1st Li-extraction /mAh g^{-1}	1st cycle efficiency /%
CNTs	822	199	24.2
Sb	1023	648	63.3
$SnSb_{0.5}$ alloy	951	726	76.3
CNTs-Sb (36wt.%)	1266	462	36.5
CNTs-$SnSb_{0.5}$ (56wt.%)	1092	518	47.4

D. Improvements in cycle efficiency

Lithium storage metals such as Sn, Sb and Pb, in spite of their significantly high electrochemical lithium intercalation capacities, develop cracks easily during applications and the crumbling of the electrode is a major cause of the observed rapid fading of their capacities. This is a consequence of the large specific volume changes in the lithiation and de-lithiation reactions. Metal-carbon composites such as Sn-C [29], SnSb-MCMB [30] and Sn-Fe-C [21] were introduced to moderate such propensity. A soft carbonaceous material can in principle be used to absorb the mechanical stress caused by the volume changes, thus improving the cyclability of the composite electrode. It has been demonstrated that the cyclability of tin and tin oxide could be substantially improved by dispersing them in graphite [31, 32]. In this work the dispersion of the metal alloy particles in the CNT web, or coating the metal alloy particles on the CNT surface, were carried out for the same purpose. A comparison of the cyclability of CNTs, Sb and $SnSb_{0.5}$ particles and their nanocomposites in electrochemical lithiation and de-lithiation

reactions is shown in Fig. 8. Low reversible capacity aside, the CNT electrode nevertheless shows rather good stability towards electrochemical cycling. The reversible capacity of CNT electrode after 50 cycles was 147 mAh/g, or 74% retention of the initial capacity. The capacity fading was very severe in unsupported Sb and $SnSb_{0.5}$ electrodes (Fig. 8). Although their peak capacities were as high as 648 mAh/g for Sb and 726 mAh/g for $SnSb_{0.5}$ respectively, the capacities fell below the level of CNT in 25 cycles for Sb and in 32 cycles for $SnSb_{0.5}$. The rapid capacity fading confirms the occurrence of uneven expansion and contraction of alloy particles during lithiation and de-lithiation reactions. The deficiency was greatly reduced after dispersing Sb and $SnSb_{0.5}$ in the CNT network, which promotes the formation of metal particles in smaller dimensions and the soft CNT also serves to absorb the mechanical stress from the volume change in repetitive charging and discharging operations. In addition, the conducting CNT network maintains the electrical connectivity of the particles even after pulverization. After 30 cycles, the capacity decreased from 462 mAh/g to 287mAh/g for the CNT-Sb electrode, and from 549 mAh/g to 369 mAh/g for the CNT-$SnSb_{0.5}$. By comparison the capacity decrease for the unsupported electrodes was from 648 mAh/g to 115 mAh/g for Sb and from 726 mAh/g to 174 mAh/g for $SnSb_{0.5}$. These experimental evidences when viewed collectively confirm that the CNT-metal composites are more cyclable than unsupported Sb and $SnSb_{0.5}$ particles, and have higher reversible capacities than CNTs.

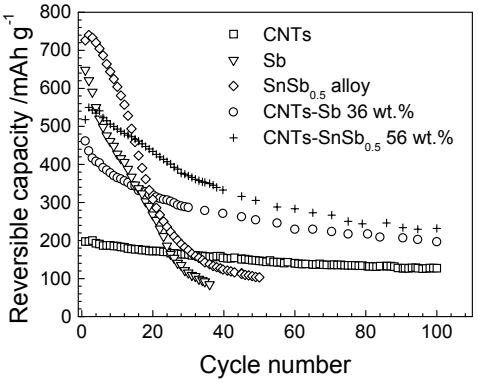

Fig. 8. Reversible capacities as a function of cycle number for CNTs, Sb, $SnSb_{0.5}$, CNT-Sb, and CNT-$SnSb_{0.5}$ electrodes at the constant current density of 50 mA/g and between 0-2.0 V.

IV. Conclusions

CNT-Sb and CNT-$SnSb_{0.5}$ nano-composites were prepared by simple chemical procedures. SEM and TEM examinations showed the presence of nanosize Sb and $SnSb_{0.5}$ particles either in the CNT web and on the outside surface of the CNTs. Besides maintaining the metal particles in nanoscale dimensions, the CNT web is also expected to be an effective buffer for the mechanical stress induced by volume changes in charging and discharging reactions, thereby reducing the particle break up in electrochemical cycling. As a result the rapid capacity fading of the metal particles was more restrained. It was found that CNT-metal nanocomposites exhibited improved cyclability compared to unsupported Sb and SnSb particles and higher reversible specific capacities than CNTs.

References

[1] C. N. R. Rao, B. C. Satishkumar, A. Govindaraj, M. Nath, "Nanotubes." *ChemPhysChem.,* vol. 2, no. 2, pp78-105, 2001.

[2] E T. Thostenson, Z. F. Ren, T. W. Chou, "Advances in the science and technology of carbon nanotubes and their composites: a review." *Comp. Sci. Tech.,* vol. 61, no. 13, pp1899-1912, 2001.

[3] T. Rueckes, K. Kim, E. Joselevich, G. Y. Tseng, C. L.Cheung, C. M. Lieber, "Carbon nanotube-based nonvolatile random access memory for molecular computing." *Science,* vol. 289, no. 5476, pp94-97, 2000.

[4] Z. Yao, H. W. C. Postma, L. Balents, C. Dekker,. "Carbon nanotube intramolecular junctions." *Nature,* vol. 402, no. 6759, pp273-276, 1999.

[5] A. C. Dillon, K. M. Jones, T. A. Bekkedahl, C. H. Kiang, D. S. Bethune, M. J. Heben, "Storage of hydrogen in single-walled carbon nanotubes." *Nature,* vol. 386, no. 6623, pp377-379, 1999.

[6] P. Chen, X. Wu, J. Lin, K. L. Tan, "High H_2 uptake by alkali-doped carbon nanotubes under ambient pressure and moderate temperatures." *Science,* vol. 285, no. 5424, pp91-93, 1999.

[7] B. S. Files, B. M. Mayeaux, "Carbon nanotubes." *Adv. Mater. Proc.,* vol. 156, no. 4, pp47-49, 1999.

[8] P. Calvert, "Nanotube composites - A recipe for strength." *Nature,* vol. 399, no. 6733, pp210-211, 1999.

[9] E. Frackowiak, S. Gautier, H. Gaucher, S. Bonnamy, F. Beguin, "Electrochemical storage of lithium multiwalled carbon nanotubes." *Carbon,* vol. 37, no. 1, pp61-69, 1999.

[10] B. Gao, A. Kleinhammes, X. P. Tang, C. Bower, L. Fleming, Y. Wu, O. Zhou, "Electrochemical intercalation of single-walled carbon nanotubes with lithium." *Chem. Phys. Lett.,* vol. 307, no. 3-4, pp153-157, 2000.

[11] G. T. Wu, C. S. Wang, X. B. Zhang, H. S. Yang, Z. F. Qi, P. M. He, W. Z. Li, "Structure and lithium insertion properties of carbon nanotubes." *J. Electrochem. Soc.,* vol. 146, no. 5, pp1696-1701, 1999.

[12] A. S. Claye, J. E. Fischer, C. B. Huffman, A. G. Rinzler, R. E. Smalley, "Solid-state electrochemistry of the Li single wall carbon nanotube system." *J. Electrochem. Soc.,* vol. 147, no. 8, pp2845-2852, 2000.

[13] K. H. An, W. S. Kim, Y. S. Park, J.M. Moon, D. J. Bae, S. C. Lim, Y. S. Lee, Y. H. Lee, "Electrochemical properties of high-power supercapacitors using single-walled carbon nanotube electrodes." *Adv. Funct. Mat.,* vol 11, no. 5, pp387-392, 2001.

[14] L. Diederich, E. Barborini, P. Piseri, A. Podesta, P. Milani, A. Schneuwly, R. Gallay, "Supercapacitors based on nanostructured carbon electrodes grown by cluster-beam deposition." *Appl. Phys. Lett.,* vol. 75, no. 17, pp2662-2664, 1999.

[15] V. A. Nalimova, D. E. Sklovsky, G. N. Bondarenko, S. Bonnamy, F. Beguin, "Lithium interaction with carbon nanotubes." *Synth. Met.,* vol.88; no. 2, pp89-93, 1997.

[16] M. Winter, J. O. Besenhard, "Electrochemical lithiation of tin and tin-based intermetallics and composites." *Electrochim. Acta.,* vol. 45, no. 1-2, pp31-50, 1999.

[17] J. Yang, Y. Takeda, N. Imanishi, O. Yamamoto, "Ultrafine Sn and $SnSb_{0.14}$ powders for lithium storage matrices in lithium-ion batteries." *J. Electrochem. Soc.,* vol. 146, no. 11, pp4009-4013, 1999.

[18] J. Yang, M. Wachtler, M. Winter, J. O. Besenhard, "Sub-microcrystalline Sn and Sn-SnSb powders as lithium storage materials for lithium-ion batteries." *Electrochem. Solid-State Lett.,* vol. 2, no. 4, pp161-163, 1999.

[19] K. D. Kepler, J. T. Vaughey, M. M. Thackeray, "$LixCu_6Sn_5$ ($0 < x < 13$): An intermetallic insertion electrode for rechargeable lithium batteries." *Electrochem. Solid State Lett.,* vol. 2, no. 7, pp307-309, 1999.

[20] R. Alcantara, F. J. Fernandez-Madrigal, P. Lavela, J. L. Tirado, J. C. Jumas, J. Olivier-Fourcade, "Electrochemical reaction of lithium with the CoSb3 skutterudite." *J. Mater. Chem.,* vol. 9, no. 10, pp2517-2521, 1999.

[21] O. Mao, R. A. Dunlap, J. R. Dahn, "Mechanically alloyed Sn-Fe(-C) powders as anode materials for Li-ion batteries- I The Sn_2Fe-C system." J. Electrochem. Soc., vol. 146, no. 2, pp405-413, 1999.

[22] M. Garreau, J. Thevenin, M. Fikir, *J. Power Sources,* vol. 9, pp235-239, 1983.

[23] J. O. Besenhard, J. Yang, M. Winter, "Will advanced lithium-alloy anodes have a chance in lithium-ion batteries?" *J. Power Sources,* vol. 68, no.1, pp87-90, 1997.

[24] N. C. Li, C. R. Martin, B. Scrosati, "A high-rate, high-capacity, nanostructured tin oxide electrode." *Electrochem. Solid State Lett.*, vol. 3, no. 7, pp316-318, 2000.

[25] N. C. Li, C. R. Martin, "A high-rate, high-capacity, nanostructured Sn-based anode prepared using sol-gel template synthesis." *J. Electrochem. Soc.,* vol. 148, no. 2, ppA164-A170, 2001.

[26] I. A. Courtney, J. R. Dahn, "Key factors controlling the reversibility of the reaction of lithium with SnO_2 and Sn_2BPO_6 glass." *J. Electrochem. Soc.,* vol. 144, no. 9, pp2943-2948, 1997.

[27] W. F. Liu, X. J. Huang, Z. X. Wang, H. Li, L. Q. Chen, "Studies of stannic oxide as an anode material for lithium-ion batteries." *J. Electrochem. Soc.,* vol. 145, no. 1, pp59-62, 1998.

[28] C. S. Wang, G. T. Wu, X. B. Zhang, Z. F. Qi, W. Z. Li, "Lithium insertion in carbon-silicon composite materials produced by mechanical milling." *J. Electrochem. Soc.,* vol. 145, no. 8, pp2751-2758, 1997.

[29] G. X. Wang, J. H. Ahn, M. J. Lindsay, L. Sun, D. H. Bradhurst, S. X. Dou, H. K. Liu, "Graphite-Tin composites as anode materials for lithium-ion batteries." *J. Power Sources,* vol. 97-8, pp211-215, 2001.

[30] L. H. Shi, H. Li, Z. X. Wang, X. J. Huang, L. Q. Chen, "Nano-SnSb alloy deposited on MCMB as an anode material for lithium ion batteries." *J. Mater. Chem.,* vol. 11, no. 5, pp1502-1505, 2001.

[31] J. Y. Lee, R. F. Zhang, Z. L. Liu, "Lithium intercalation and deintercalation reactions in synthetic graphite containing a high dispersion of SnO." *Electrochem. Solid State Lett.,* vol. 3, no. 4, pp167-170, 2000.

[32] J. Y. Lee, R. F. Zhang, Z. L. Liu, "Dispersion of Sn and SnO on carbon anodes." *J. Power Sources,* vol. 90, no. 1, pp70-75, 2001.

[33] Y. Zhang, N. W. Franklin, R. J. Chen, H. J. Dai, "Metal coating on suspended carbon nanotubes and its implication to metal-tube interaction." *Chem. Phys. Lett.,* vol. 331, no. 1, pp35-41, 2000.